



Substituent and metal effects on C—C σ -complex stabilization

Yumeng Cao, Dean J. Tantillo*

Department of Chemistry, University of California—Davis, Davis 95616, CA, United States

ARTICLE INFO

Keywords:

Sigma complex
Donor-acceptor interaction
3-center 2-electron bonding
Non-classical
DFT

ABSTRACT

Three-center, two-electron bonding arrays in σ -complexes between C—C bonds and transition metals were examined using density functional theory computations. Variations in ligands and metals were connected to variations in strengths of bonding interactions in these arrays.

1. Introduction

The interaction between transition metal complexes and σ -bonds results in so-called σ -complexes, held together by three-center, two-electron bonding arrays [1–4]. These bonding units arise from the donation of electrons from a σ -bond to a vacant orbital on the transition metal. σ -Complexes are considered to be key intermediates in C—H and C—C bond activation processes [5]. We were intrigued by previous reports of isolable σ -complexes involving interactions between C—C σ -bonds and rhodium (Fig. 1) [5–8]. Building on seminal computational work from the Weller group [7,8], we used density functional theory (DFT) to explore this type of structure here, along with variations involving different ligands, transition metals, and other possible bridging groups.

The orbital interactions leading to the three-center, two-electron bonds in σ -complexes are shown qualitatively in Fig. 2. Stabilization arises through both the interaction of the filled C—C σ orbital a vacant metal-X σ^* -orbital (sometimes formulated simply as a p-orbital on the metal) – to which we refer as a σ -type interaction – and the interaction of a filled metal d orbital with the vacant C—C σ^* orbital – to which we refer as a π -type interaction [2].

2. Computational methods

All calculations were performed using Gaussian 16 Revision C.01 [9]. Structure optimizations and frequency analyses were carried out with the PBE0 functional [10,11] and the def2-SVP basis set, and single-point energies were calculated using the def2-TZVP basis set [12]. This approach was chosen based on previous studies showing that this level of theory is effective for accurately calculating C—C activation mechanisms [13]. While the Weller group previous used Atoms-In-Molecules (AIM) methods to characterize bonding in the types of σ -complexes examined here [7,8], we made use of Mayer bond orders [14] (determined using the Multiwfn software package version 3.8 (dev)) [15,16] and Natural Bond Orbital (NBO) [18] analyses (carried out with NBO 7.0) [19]. Conformational searches were conducted with CREST (Conformer-Rotamer Ensemble Sampling Tool) [17].

3. Results and discussion

We first explored how the R group on the phosphine ligand affects the stabilization of the σ -complex (Fig. 3a). We calculated the Natural Bond Orbital (NBO) interaction energies for the σ -type and π -type interactions (Fig. 3b), and the former were consistently dominant. While

* Corresponding author.

E-mail address: djtantillo@ucdavis.edu (D.J. Tantillo).

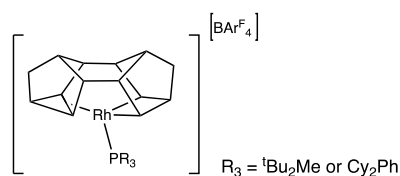


Fig. 1. Structure for analysis in this study.

sensitivity to the identity of the alkyl group on the phosphine ligands was not observed, substituting these groups with hydrogen enhances the interaction strength. Suspecting that this effect resulted from a better energy match between the interacting orbitals with PH_3 , we examined the frontier molecular orbitals (FMOs) associated with each interaction (Fig. 4 left), which validated this simple conjecture.

Bond lengths and Mayer bond orders for each complex are summarized in Fig. 3c-d. Although the NBO interaction energy increases when the R group on the phosphine ligand is hydrogen, the Mayer bond order between Rh and carbon decreases. However, the bond order between Rh and phosphorus increases. The geometries of each complex with key distances are shown in Fig. 3d.

Next, we investigated how the transition metal itself influences the stabilization of the σ -complex by substituting rhodium with cobalt and iridium (Fig. 5a). The NBO interaction energies, bond lengths, and Mayer bond orders are summarized in Fig. 5b-d. As the metal is replaced by those lower in the periodic table, NBO interaction energies within the three-center, two-electron array increase (Fig. 5b). However, examining the FMO energies shows that the energy match for σ -type interaction worsens concomitantly (Fig. 6 left), suggesting that the increase in interaction strength is likely a result of enhanced orbital overlap.

For the cobalt complex (and only this complex), the triplet configuration is approximately 22 kcal/mol lower in energy than the singlet configuration (Fig. 7). However, the geometry of the triplet state differs significantly from the singlet, with the metal positioned much closer to the center of the hydrocarbon framework. The unpaired spins in this structure are localized on the metal (Fig. 7, right).

Next, we replaced the transition metals with main group non-metals, including boron, carbon, silicon, and germanium, to determine whether three-center two-electron arrays might persist in these structures [20, 21]. Our hope was to build bridges between transition metal, main group and organic chemistry. However, when the metals were replaced by CCH_3 or CH , the structure rearranged (Fig. 8, top). These structures

contain cyclic three-center two-electron arrays, but they are not located in the molecule's center. The results for other main group-containing structures are shown in Fig. 9. While the BH-containing species does not delocalize much, the SiH- and GeH-containing species do. Both display strong σ -type interactions (but of course lack π -type interactions). Additional minor orbital interactions also contribute (see supporting information for details). The observed orbital interaction trends are again consistent with FMO energy gaps (Fig. 10).

Finally, we evaluated the energy required to transfer the metal group from one side of the hydrocarbon framework to the other. As shown in Fig. 11, this process actually requires two steps, with the intermediacy of an approximately symmetrically bridged intermediate. This intermediate (whose wavefunction appears to be stable; i.e., lacks diradical character) resides on a flat portion of the free energy surface, however. The overall free energy barrier for transferring the metal group is predicted to be approximately 10–11 kcal/mol, suggesting that this process is fast. The Weller group previously predicted a similar scenario [8].

4. Conclusion

The factors influencing the stability of σ -complexes were evaluated by examining the effects of substituents on phosphine ligands, different transition metals, and main group non-metals, starting from an isolable σ -complex model. Our results indicate that the identity of the ligand and metal can indeed modulate the interactions in these complexes, sometimes opening up additional reaction pathways involving diradicals and rearranged frameworks. Straightforward FMO arguments appear to work well for these systems.

CRediT authorship contribution statement

Yumeng Cao: Writing – review & editing, Writing – original draft, Visualization, Investigation, Data curation. **Dean J. Tantillo:** Writing – review & editing, Supervision, Resources, Project administration, Funding acquisition, Conceptualization.

Declaration of competing interest

The authors declare the following financial interests/personal relationships which may be considered as potential competing interests: Dean J. Tantillo reports financial support was provided by National Science Foundation. If there are other authors, they declare that they

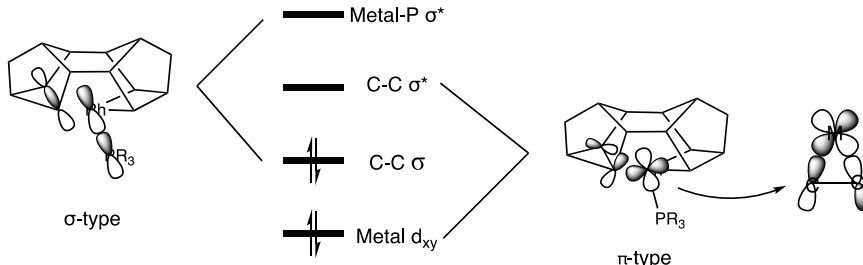
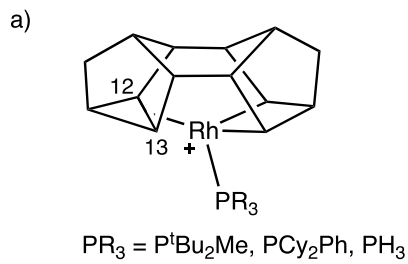


Fig. 2. Orbital interaction representation for three-center, two electron complexes.



b)

PR_3	σ -type (kcal/mol)	π -type (kcal/mol)
$\text{P}^t\text{Bu}_2\text{Me}$	20.79	4.54
PCy_2Ph	21.31	4.90
PH_3	35.28	5.96

c)

PR_3	Bond Length (Å)			Mayer Bond Order			
	C12-C13	C12-Rh	C13-Rh	C12-C13	C12-Rh	C13-Rh	Rh-P
$\text{P}^t\text{Bu}_2\text{Me}$	1.60	2.38	2.35	0.83	0.17	0.21	0.71
PCy_2Ph	1.60	2.34	2.35	0.83	0.21	0.19	0.56
PH_3	1.61	2.30	2.30	0.95	0.08	0.08	0.98

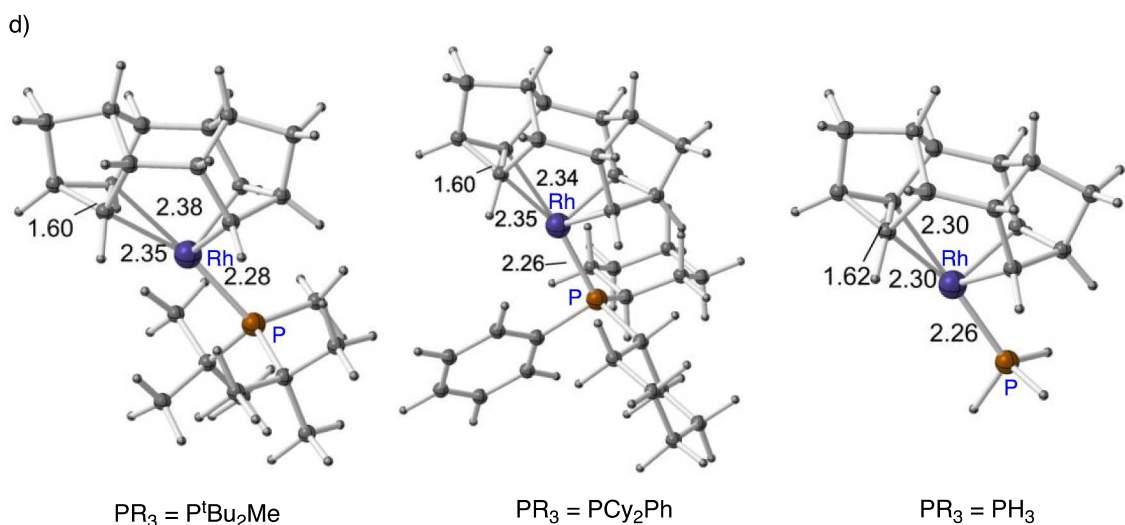


Fig. 3a). Structures analyzed. b) NBO interaction energies for each structure. c) Bond lengths and Mayer bond orders in σ -complexes with different R groups. d) Optimized geometries of σ -complexes and selected distances (Å).

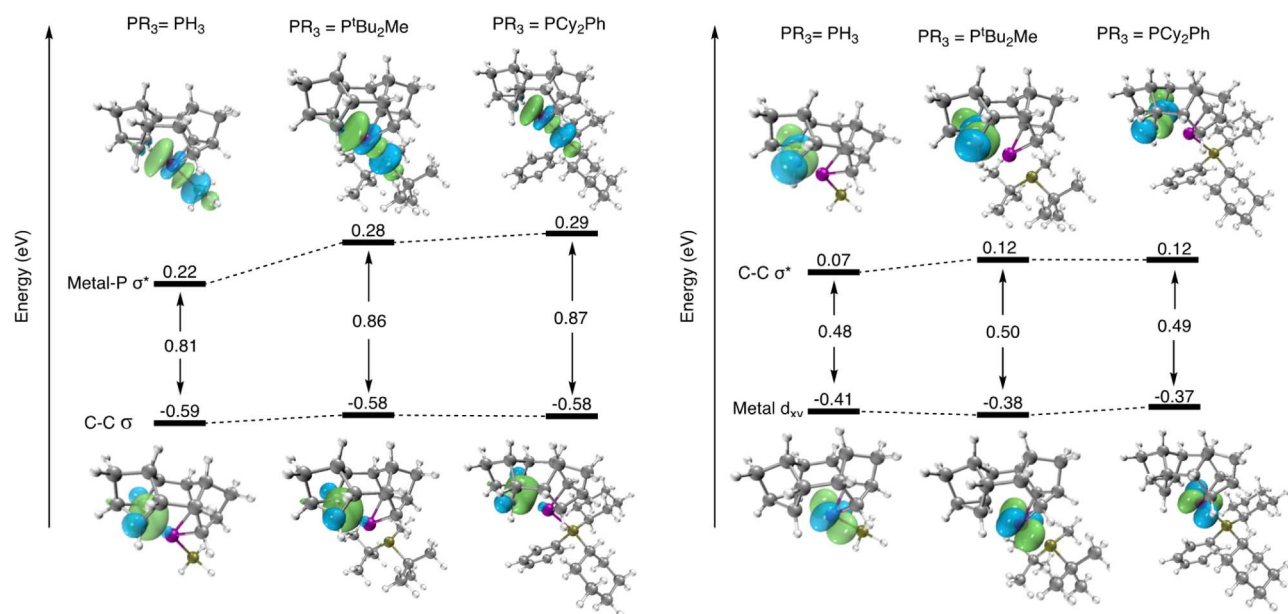


Fig. 4. Frontier molecular orbitals and orbital energy gaps for σ -complexes with PtBu_2Me , PCy_2Ph , and PH_3 ligands. The figure on the left corresponds to σ -type bonding, while the figure on the right corresponds to π -type bonding.

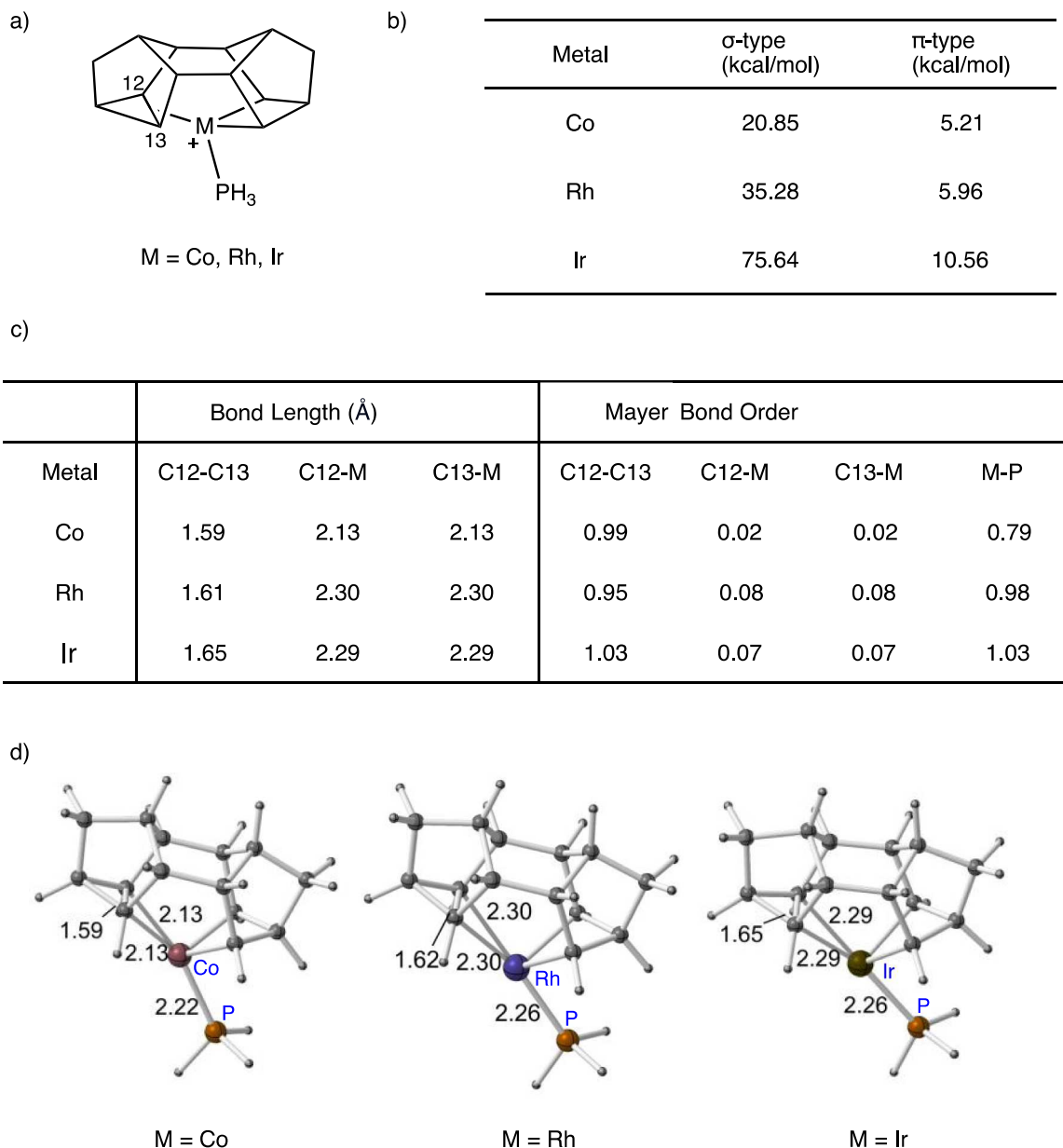


Fig. 5a). Structures analyzed. b) NBO interaction energies for each structure. c) Bond lengths and Mayer bond orders in σ -complexes with different metals. d) Optimized geometries of σ -complexes and selected distances (Å).

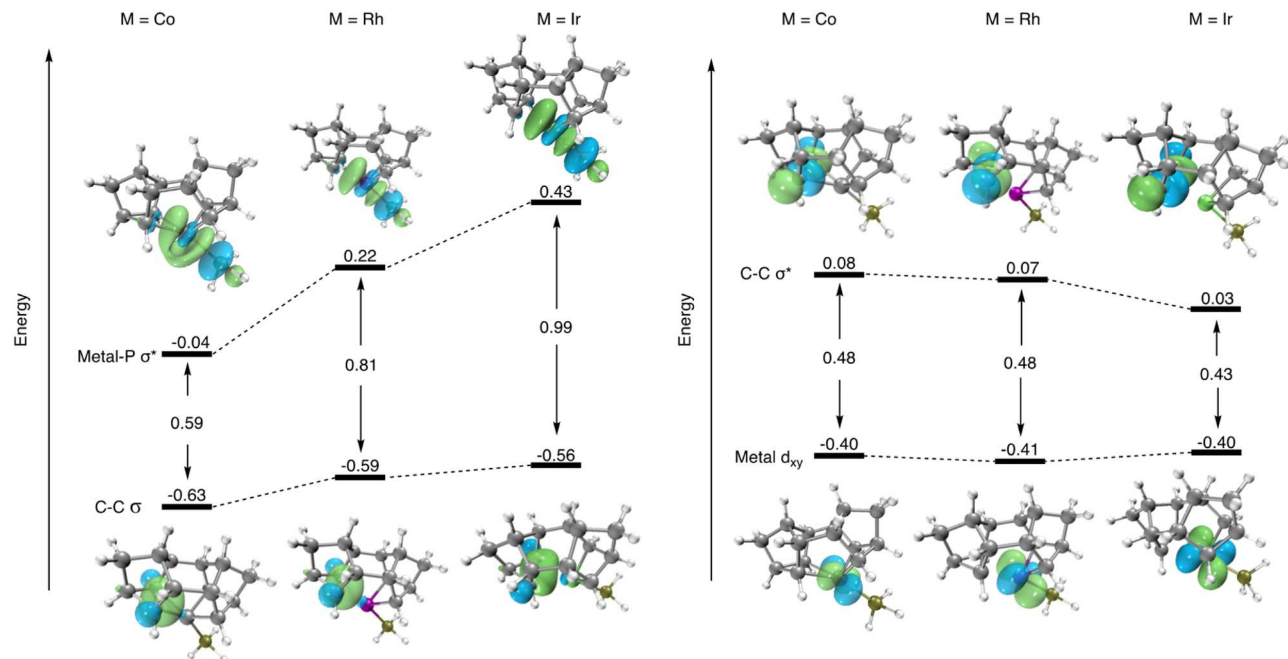


Fig. 6. Frontier molecular orbitals and orbital gaps for different structure with different metals, including Co, Rh, and Ir. The figure on the left represents the interaction involving the σ -type, while the figure on the right represents the interaction involving the π -type.

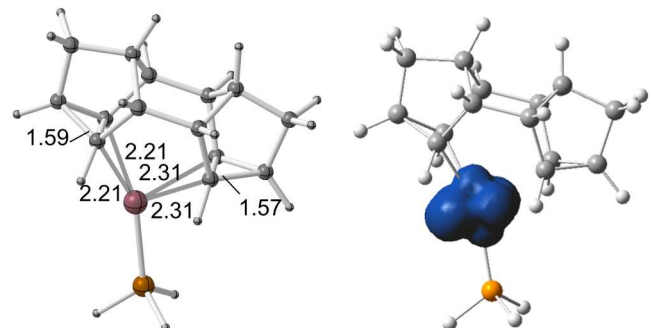


Fig. 7. Geometry for triplet with Co (left) and spin density surface for this molecule (right).

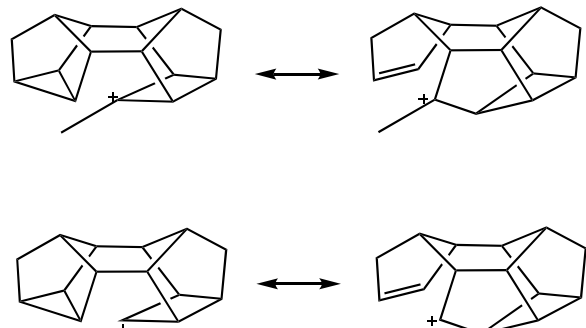


Fig. 8. Rearranged structures obtained when transition metal was replaced with carbon.

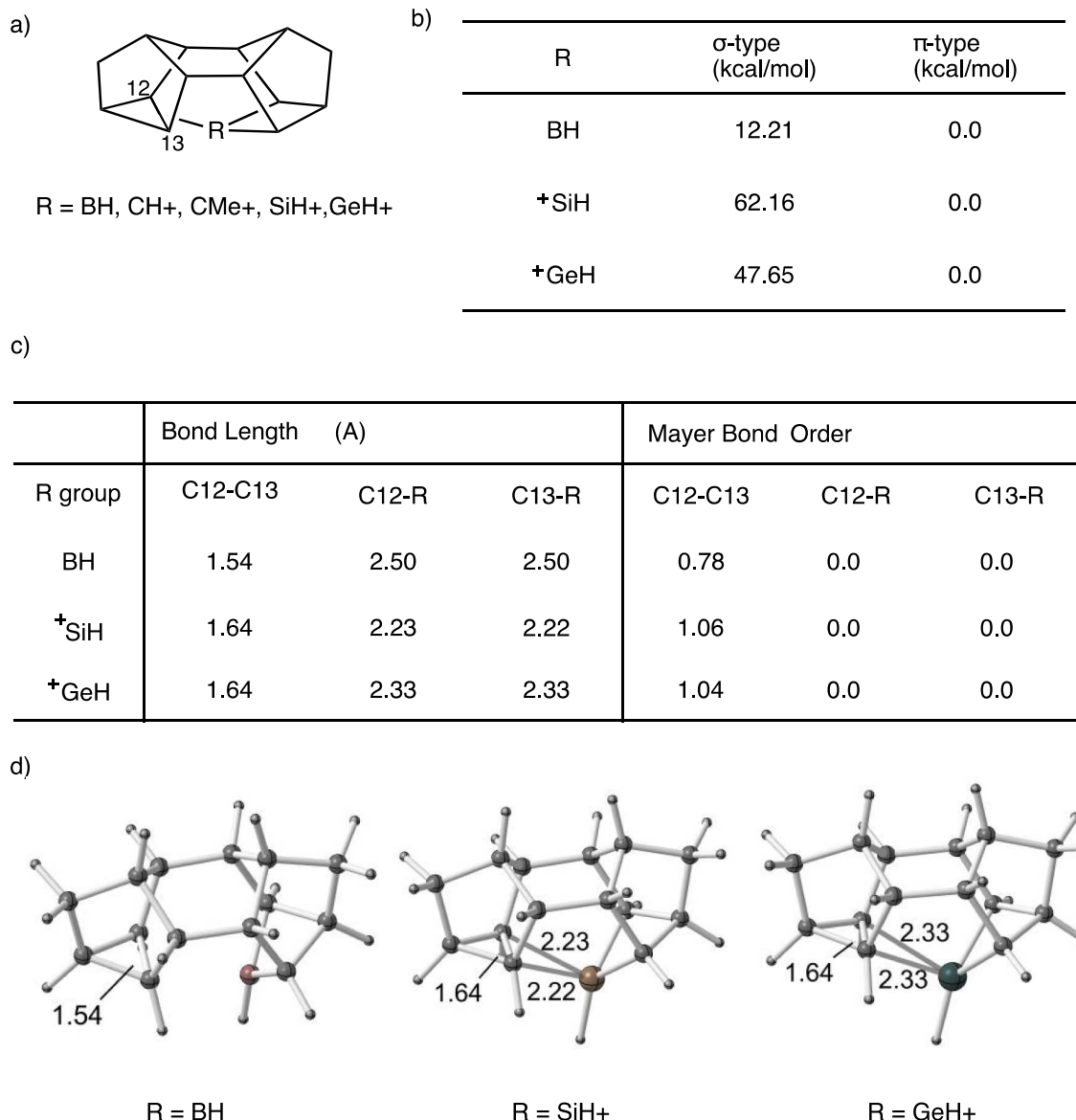


Fig. 9a). Structures analyzed here. b) NBO interaction energies for each structure. c) Bond lengths and Mayer bond orders. d) Optimized geometries and selected distances (Å).

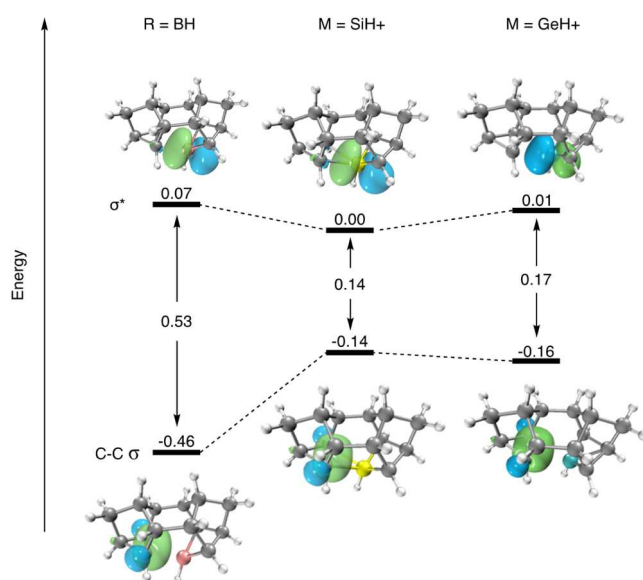


Fig. 10. Frontier molecular orbitals and orbital gaps for σ -type in different complexes.

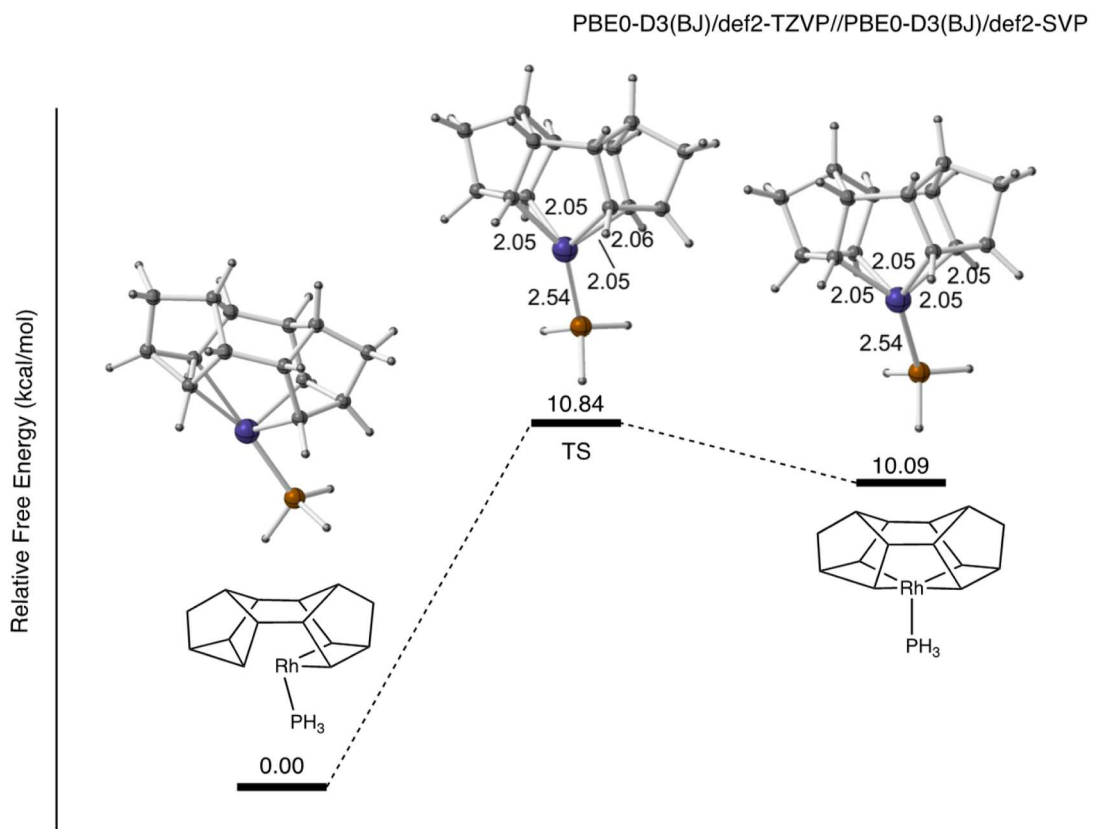


Fig. 11. Energy profile for translating the metal group from one side of the hydrocarbon framework to the other.

have no known competing financial interests or personal relationships that could have appeared to influence the work reported in this paper.

Acknowledgement

We are grateful for financial (CHE-2154083) and computational (ACCESS, CHE-030089) support from the NSF. This paper is dedicated to Thomas Strassner.

Supplementary materials

Supplementary material associated with this article can be found, in the online version, at [doi:10.1016/j.jorgchem.2024.123414](https://doi.org/10.1016/j.jorgchem.2024.123414) [22].

Data availability

Data is available at <https://iochem-bd.bsc.es/browse/review-collection/100/328,327/a50b55a255ea4d3c69dc7f4f>

References

- [1] A.S. Weller, F.M. Chadwick, A.I. McKay, Chapter five - transition metal alkane-sigma complexes: synthesis, characterization, and reactivity, *Adv. Organomet. Chem.* (2016) 223–276, <https://doi.org/10.1016/bs.adomc.2016.09.001>.
- [2] B. Rybitchinski, D. Milstein, Metal insertion into C–C bonds in solution, *Angew. Chem. Int. Ed.* 38 (1999) 870–883, [https://doi.org/10.1002/\(SICI\)1521-3773\(19990401\)38:7<870::AID-ANIE870>3.0.CO;2-3](https://doi.org/10.1002/(SICI)1521-3773(19990401)38:7<870::AID-ANIE870>3.0.CO;2-3).
- [3] G.J. Kubas, Metal Dihydrogen and σ -Bond Complexes: Structure Theory and Reactivity, Springer US, Boston, MA, 2001, <https://doi.org/10.1007/b113929>.
- [4] C. Hall, R.N. Perutz, Transition metal alkane complexes, *Chem. Rev.* 96 (1996) 3125–3146, <https://doi.org/10.1021/cr9502615>.
- [5] A.B. Chaplin, J.C. Green, A.S. Weller, C.C. Activation in the Solid State in an Organometallic σ -Complex, *J. Am. Chem. Soc.* 133 (2011) 13162–13168, <https://doi.org/10.1021/ja2047599>.
- [6] A.B. Chaplin, A.S. Weller, The influence of phosphine cone angle on the synthesis and structures of $[\text{Rh}(\text{PR}_3)(\text{Binor-S})]^+$ complexes that show C–C sigma interactions, *J. Organomet. Chem.* 730 (2013) 90–94, <https://doi.org/10.1016/j.jorgchem.2012.09.013>.
- [7] S.K. Brayshaw, J.C. Green, G. Kociok-Köhne, E.L. Sceats, A.S. Weller, A rhodium complex with one Rh $\bullet\bullet$ C and one Rh $\bullet\bullet$ H-C agostic bond, *Angew. Chem. Int. Ed. Engl.* 45 (2006) 452–456, <https://doi.org/10.1002/anie.200503036>.
- [8] S.K. Brayshaw, E.L. Sceats, J.C. Green, A.S. Weller, C–C σ complexes of rhodium, *Proc. Natl. Acad. Sci.* 104 (2007) 6921–6926, <https://doi.org/10.1073/pnas.0609824104>.
- [9] Gaussian 16, Revision C.01, M.J. Frisch, G.W. Trucks, H.B. Schlegel, G.E. Scuseria, M.A. Robb, J.R. Cheeseman, G. Scalmani, V. Barone, G.A. Petersson, H. Nakatsuji, X. Li, M. Caricato, A.V. Marenich, J. Bloino, B.G. Janesko, R. Gomperts, B. Mennucci, H.P. Hratchian, J.V. Ortiz, A.F. Izmaylov, J.L. Sonnenberg, D. Williams-Young, F. Ding, F. Lipparini, F. Egidi, J. Goings, B. Peng, A. Petrone, T. Henderson, D. Ranasinghe, V.G. Zakrzewski, J. Gao, N. Rega, G. Zheng, W. Liang, M. Hada, M. Ehara, K. Toyota, R. Fukuda, J. Hasegawa, M. Ishida, T. Nakajima, Y. Honda, O. Kitao, H. Nakai, T. Vreven, K. Throssell, J.A. Montgomery, Jr., J.E. Peralta, F. Ogliaro, M.J. Bearpark, J.J. Heyd, E.N. Brothers, K.N. Kudin, V.N. Staroverov, T.A. Keith, R. Kobayashi, J. Normand, K. Raghavachari, A.P. Rendell, J.C. Burant, S.S. Iyengar, J. Tomasi, M. Cossi, J.M. Millam, M. Klene, C. Adamo, R. Cammi, J.W. Ochterski, R.L. Martin, K. Morokuma, O. Farkas, J.B. Foresman, and D.J. Fox, Gaussian, Inc., Wallingford CT, 2016.
- [10] C. Adamo, V. Barone, Toward reliable density functional methods without adjustable parameters: the PBE0 model, *J. Chem. Phys.* 110 (1999) 6158–6170, <https://doi.org/10.1063/1.478522>.
- [11] S. Grimme, J. Antony, S. Ehrlich, H. Krieg, A consistent and accurate ab initio parametrization of density functional dispersion correction (DFT-D) for the 94 elements H–Pu, *J. Chem. Phys.* 132 (2010) 154104, <https://doi.org/10.1063/1.3382344>.
- [12] F. Weigend, R. Ahlrichs, Balanced basis sets of split valence, triple zeta valence and quadruple zeta valence quality for H to Rn: design and assessment of accuracy, *Phys. Chem. Chem. Phys.* 7 (2005) 3297, <https://doi.org/10.1039/b508541a>.
- [13] N. Jha, W. Guo, W.Y. Kong, D.J. Tantillo, M. Kapur, Regiocontrol via Electronics: Insights into a Ru-Catalyzed, Cu-Mediated Site-Selective Alkylation of Isoquinolones via a C–C Bond Activation of Cyclopropanols, *Chem. – Eur. J.* 29 (2023) e202301551, <https://doi.org/10.1002/chem.202301551>.
- [14] A.J. Bridgeman, G. Cavigliasso, L.R. Ireland, J. Rothery, The Mayer bond order as a tool in inorganic chemistry, *J. Chem. Soc. Dalton Trans.* (2001) 2095–2108, <https://doi.org/10.1039/b102094n>.
- [15] T. Lu, F. Chen, Multiwfn: a multifunctional wavefunction analyzer, *J. Comput. Chem.* 33 (2012) 580–592, <https://doi.org/10.1002/jcc.22885>.
- [16] T. Lu, A comprehensive electron wavefunction analysis toolbox for chemists, Multiwfn, *J. Chem. Phys.* 161 (2024) 082503, <https://doi.org/10.1063/5.0216272>.
- [17] P. Pracht, S. Grimme, C. Bannwarth, F. Bohle, S. Ehlert, G. Feldmann, J. Gorges, M. Müller, T. Neudecker, C. Plett, S. Spicher, P. Steinbach, P.A. Wesolowski, F. Zeller, CREST—A program for the exploration of low-energy molecular chemical space, *J. Chem. Phys.* 160 (2024) 114110, <https://doi.org/10.1063/5.0197592>.
- [18] F. Weinhold, Natural bond orbital analysis: a critical overview of relationships to alternative bonding perspectives, *J. Comput. Chem.* 33 (2012) 2363–2379, <https://doi.org/10.1002/jcc.23060>.
- [19] NBO 7.0, E.D. Glendening, J. K. Badenhoop, A.E. Reed, J.E. Carpenter, J.A. Bohmann, C.M. Morales, P. Karafiloglou, C.R. Landis, and F. Weinhold, Theoretical Chemistry Institute, University of Wisconsin, Madison (2018), (n.d.).
- [20] H.C. Brown, *The Nonclassical Ion Problem*, Springer Science & Business Media, 2012.
- [21] C. Walling, An innocent bystander looks at the 2-norbornyl cation, *Acc. Chem. Res.* 16 (1983) 448–454, <https://doi.org/10.1021/ar00096a004>.
- [22] M. Álvarez-Moreno, C. de Graaf, N. López, F. Maseras, J.M. Poblet, C. Bo, Managing the computational chemistry big data problem: the ioChem-BD platform, *J. Chem. Inf. Model.* 55 (2015) 95–103, <https://doi.org/10.1021/ci500593j>.